Pergamon

Acta mater. 49 (2001) 583–588

Acta MATERIALIA

www.elsevier.com/locate/actamat

KINETIC MODEL OF LOW PRESSURE FILM DEPOSITION FROM SINGLE PRECURSOR VAPOR IN A WELL-MIXED, COLD-WALL REACTOR

S. KRUMDIECK*

Department of Mechanical Engineering, University of Colorado at Boulder, Campus Box 427, Boulder, CO 80309, USA

(Received 29 May 2000; received in revised form 18 October 2000; accepted 23 October 2000)

Abstract—A phenomenological model was derived to describe the deposition kinetics of oxide film growth from thermally activated decomposition of vapor precursor on a heated surface at low pressure. A Langmuir derivation of mass balance on the growing film surface with surface saturation condition was used to model the deposition. Growth rate of solid oxide film was modeled as a function of molecular arrival rate, adsorption rate, and surface reaction rate. The model was applied to a novel metalorganic chemical vapor deposition process (Pulsed-MOCVD). The process features precisely controlled pulsed injection of precursor solution with ultrasonic atomization to deliver the precursor vapor to the reactor with no carrier gas. Growth behavior was predicted for an experimental investigation in which a dilute solution of $Ti(OPr)_4$ (isopropoxide) in toluene was used as the liquid precursor for TiO_2 rutile film on nickel substrate. © *2001 Acta Materialia Inc. Published by Elsevier Science Ltd. All rights reserved.*

Keywords: Chemical vapor deposition (CVD); Theory & modeling; Kinetics; Thin films

1. INTRODUCTION

Most CVD systems which have been modeled are either high pressure, diffusion controlled processes [1–3] or low pressure kinetic controlled processes [4–7]. The unique precursor delivery system employed in the Pulsed-MOCVD process results in reactor conditions which fluctuate between molecular flow and viscous flow within a 10 s time period. We used the Langmuir analysis of surface adsorption coupled with reaction kinetics to derive a phenomenological model of film growth encompassing both control regimes. The model was developed for single component, heterogeneous, thermally activated reactions in a low pressure reactor.

The motivation for this work is the patented Pulsed-MOCVD process [8] which operates in a manner fundamentally different from typical CVD [9]. Figure 1 schematically illustrates the experimental Pulsed-MOCVD system. The typical CVD carrier gas and bubbler delivery system is replaced with pulsed liquid delivery and ultrasonic atomization. Each pulse cycle delivers an exact amount of liquid precursor solution to the reactor through the ultrasonic nozzle. Precise control of injection rate is achieved without a liquid pump or mass flow controllers by using a computer to alternately actuate the solenoid valves B and C. The volume of precursor solution in tube

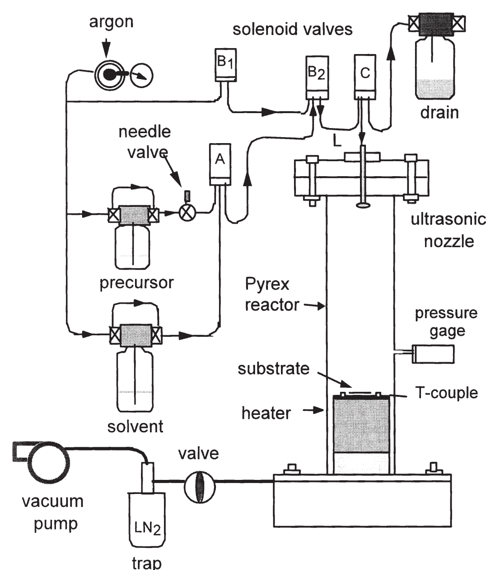

Fig. 1. Schematic representation of the Pulsed-MOCVD process. A computer controls the solenoid valves, B1, B2, and C to deliver a liquid pulse equal to the volume in tube L to the ultrasonic nozzle.

* To whom all correspondence should be addressed. At: University of Canterbury, PB 4800, Christchurch, New Zealand. Tel.: +64-3-364-9878; fax: +64-3-364-6078.

E-mail address: s.krumdieck@mech.canterbury.ac.nz (S. Krumdieck)

1359-6454/01/$20.00 © 2001 Acta Materialia Inc. Published by Elsevier Science Ltd. All rights reserved.
PII: S1359-6454(00)00356-6

length L is delivered to the ultrasonic nozzle at the desired pulse interval [10, 11]. The injection rate of precursor to the reactor is further controlled by adjusting the concentration of metal alkoxide in the solution. Solutions of a high volatility solvent, i.e. toluene, and up to 20% volume of precursor were used.

The Knudsen number ranges between 0.001 and 0.15 during each pulse, and the time constant for steady flow is typically less than 2 s at the end of each 10 s pulse cycle. These conditions make modeling by ordinary viscous flow analysis quite problematic. Our approach is to model the flow through the vertical reactor as well-mixed plug flow. At the beginning of each pulse, the precursor evaporates instantaneously, filling the reactor with a homogeneous mixture of vapor. As the reactor is pumped back down during the rest of the pulse, it is assumed that the vapor in the reactor remains well-mixed, that is, that no precursor concentration gradients develop. Since most of the film deposition occurs in the first few seconds of each pulse when the precursor partial pressure is highest, the assumption of a well-mixed vapor should be reasonably accurate. The significant processing parameters are substrate surface temperature, T_s, reactor total pressure which is a function of time through each pulse, $P(t)$, and precursor solution molar concentration, c_{mo}. The reaction activation energy, E_A, and the adsorption energy, Q, are determined by the precursor chemistry.

2. DERIVATION OF THE KINETIC DEPOSITION MODEL

The phenomenological model of the growth kinetics is derived from the conservation of mass on the surface and the physics of molecular adsorption. Thus, the model describes the deposition of a single phase solid oxide from the thermal decomposition surface reaction of a single precursor. Figure 2 shows the schematic representation of the deposition process. We assume that only physical adsorption occurs and that the low reactor pressure is below the precursor condensation pressure. If there were no attractive forces between the precursor vapor molecules and the surface, then the residence time on the surface would be of the order of the molecular vibration time, τ_o (10^{-12} to 10^{-13} s). However, if attractive forces do exist, then the Frenkel equation [12] gives the average residence time:

$$\tau = \tau_o \exp(Q/RT_s) \tag{1}$$

where τ is the residence time, Q is the adsorption energy, R is the universal gas constant, and T_s is the surface temperature. If τ is equal to several vibration cycles, then adsorption has occurred, the precursor molecule has time to be heated, and thermally activated reactions take place. For physical adsorption, Q is in the range of 5–50 kJ/mole, and τ is in the range of 10^{-12} to 4×10^{-7} s (at 25°C).

The Langmuir derivation [12] is essentially a mass balance on the surface coupled with the saturation condition, where the decomposition rate, J_D, equals the adsorption rate, J_A, minus the evaporation rate, J_E:

$$J_D = J_A - J_E \tag{2}$$

Each of the rates has units of number of molecules per second and can be expressed as the number of participating molecular sites times a rate constant, k_i:

$$\begin{aligned} J_A &= S_0 c_{mo} P(t) k_2 \\ J_D &= S_1 k_1 \\ J_E &= S_1 k_3 \end{aligned} \tag{3}$$

where S_1 is the number of precursor occupied sites and S_0 is the number of available adsorption sites, k_1 is the decomposition reaction rate, k_2 is the molecular arrival rate, and k_3 is the evaporation rate (i.e. the inverse of the adsorption rate). The total number of adsorption sites, S, is determined from the deposition area, A_s, and the area per site, σ^{mo}, which is approximated by the precursor molecular area.

$$S = \frac{A_s}{\sigma^{mo}} = S_1 + S_0 \tag{4}$$

Assuming a first order reaction, the decomposition rate constant can be expressed as:

$$k_1 = \left(\frac{1}{\tau_{10}}\right)\exp(-E_A/RT_s) \tag{5}$$

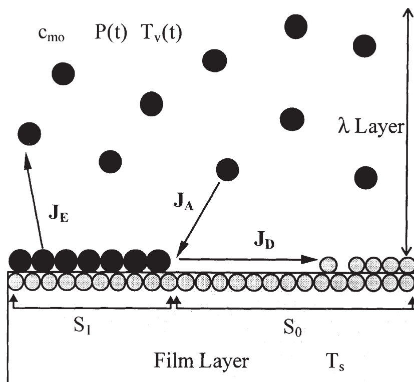

Fig. 2. Langmuir derivation of surface reaction kinetics with saturation condition and mass balance. ●, precursor molecule; ○, oxide molecule. T_s, and T_v are surface and vapor temperature, c_{mo} is precursor molar concentration, P is the reactor pressure, and λ is the mean free path.

where τ_{10} is the reactant residence time, and E_A is the reaction activation energy.

The arrival rate is a function of the process parameters, precursor concentration, c_{mo}, and reactor pressure, $P(t)$. The arrival rate constant, k_2 in molecules per second is given by kinetic gas theory. It represents the number of impacting molecules originating from within a vapor layer with thickness equal to the molecular mean free path (termed the λ-layer) that stick:

$$k_2 = \frac{\alpha N_o \sigma^{mo}}{\sqrt{2\pi M R T_v(t)}} \tag{6}$$

where α is the sticking coefficient (between 0 and 1), N_o is Avagadro's number, M is the mass per mole, and $T_v(t)$ is the vapor temperature which is a function of time in the region near the substrate.

The evaporation rate constant is simply the inverse of the adsorption time as given in equation (1):

$$k_3 = \left(\frac{1}{\tau_{30}}\right)\exp(-Q/RT_s) \tag{7}$$

Where τ_{30} is the molecular residence time. The quantity of interest in MOCVD is the film growth rate. The film growth rate is determined by the decomposition rate, J_D, the solid oxide molecular volume, Ω_{ox}, and the susceptor area:

$$\mathrm{GR} = S_1 k_1 \Omega_{ox}/A_s \tag{8}$$

The deposition rate at any given instant is given by combining the equilibrium equation (2) with the saturation equation (4), substituting in the expressions for arrival, reaction and evaporation rates (3), and solving for deposition rate as a function of surface temperature, precursor solution molar concentration, and reactor pressure:

$$\mathrm{GR}(t) = \frac{\Omega_{ox}}{\sigma^{mo}} \frac{k_1 c_{mo} P(t) k^2}{[k_1 + c_{mo}P(t)k_2 + k_3]} \tag{9}$$

The simple model can be used to describe a wide range of reactor geometries and deposition conditions by normalizing the growth rate with the maximum growth rate. The maximum growth rate, GR_{max}, would occur if every arriving precursor molecule were deposited.

$$\mathrm{GR}(t)_{max} = \frac{\Omega_{ox}}{\sigma^{mo}} c_{mo} P(t) k_2 \tag{10}$$

$$\mathrm{NGR}(t) = \frac{k_1}{k_1 + c_{mo}P(t)k_2 + k_3} \tag{11}$$

Equation (10) gives the normalized growth rate, NGR, at any time during the pulse cycle. The equation is valid as long as well-mixed reactor conditions exist.

2.1. Adaptation of the model for Pulsed-MOCVD

In the preceding analysis, the molecular arrival rate was modeled as a function of the precursor partial pressure, $c_{mo}P(t)$, assuming a well-mixed vapor. The pulsed injection delivery system is unsteady with a short time constant, so that significant concentration gradients are assumed not to develop. Thus, the growth rate is effectively controlled by the precursor injection rate and the substrate temperature. Since we have no measurements of vapor concentration gradients to verify that Pulsed-MOCVD functions as a well-mixed reactor, we will compare film growth rate measurements to the model.

Figure 3 shows a schematic diagram of the tubular vertical cold-wall reactor. The ultrasonic atomization and evaporation of droplets occurs in less than 5 μs [11]. The liquid injection process is modeled as producing well mixed precursor vapor which occupies the volume of the reactor above the susceptor at the beginning of each pulse cycle, when $t = 0$.

Molecules which impinge on the surface without further interaction with other vapor molecules originate from within a vapor layer, termed the λ-layer, equal in thickness to one mean free path. During typical operation, with a 10 s pulse period, the mean free path will vary from 1 mm to 10 mm. Heating of the precursor vapor also occurs within the λ-layer. The temperature within the λ-layer, $T_v(t)$, is assumed to be uniform because of limited intermolecular interaction. At the beginning of the pulse, the vapor evapor-

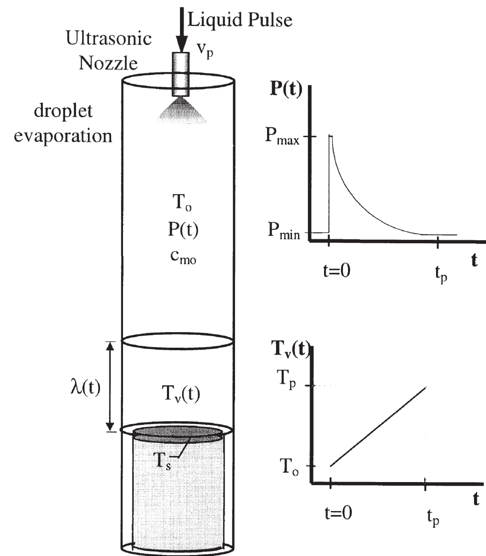

Fig. 3. Schematic drawing of the model vertical tube cold-wall reactor with vapor modeled as a well mixed reactor. Reactor pressure, $P(t)$, and the bulk vapor temperature within the λ-layer, $T_v(t)$, are shown during one pulse.

ates in the vacuum, and $T_v(t)$ is equal to T_o. By the end of the cycle, $T_v(t)$ is equal to a final temperature, T_p. Constant substrate temperature and precursor concentration through each pulse period are assumed. The vapor temperature during a pulse of length t_p is approximated by:

$$T_v(t) = T_o + \left(\frac{T_p - T_o}{t_p}\right)\cdot t \tag{12}$$

The small (<20 μm diameter) droplets from the ultrasonic nozzle evaporate quickly producing a pressure pulse, P_{max}. By the end of the pulse, the reactor is pumped down to P_{min}. The resulting pressure profile is approximated by:

$$P(t) = P_{min} + \Delta P \exp\left(-\frac{t}{\tau_p}\right) \tag{13}$$

where $\Delta P = (P_{max} - P_{min})$, and τ_p is the vacuum pump constant which was experimentally determined.

In the experimental set-up, the molar concentration of the precursor, c_{mo}, and the volume of precursor solution injected per pulse, v_p, can be varied. The injection rate of precursor in moles per pulse, Inj, is defined by:

$$\mathrm{Inj} = c_{mo}\rho_{sol}v_p \tag{14}$$

where ρ_{sol} is the molar density of the solvent. The molar injection rate is a convenient measure of precursor supply rate.

The growth rate per unit area in microns per pulse is found by integrating equations (9)–(11) with time over one pulse period.

$$\mathrm{GR}_{pulse}(T_s) = \int_0^{t_p} \mathrm{GR}(T_s,t)\mathrm{d}t \tag{15}$$

$$= \int_0^{t_p} \frac{\Omega_{ox}}{\sigma^{mo}} \frac{k_2(t)c_{mo}P(t)k_3}{[k_1(T_s) + k_2(t)c_{mo}P(t) + k_3(T_s)]}\mathrm{d}t$$

$$\mathrm{GR}_{max} = \frac{\Omega_{ox}}{\sigma^{mo}}\int_0^{t_p} c_{mo}P(t)k_2(t)\mathrm{d}t \tag{16}$$

$$\mathrm{NGR}(T_s) = \int_0^{t_p} \frac{k_1(T_s)}{k_1(T_s) + c_{mo}P(t)k_2(t) + k_3(T_s)}\mathrm{d}t \tag{17}$$

3. RESULTS: COMPARISON OF THE MODEL TO PULSED-MOCVD EXPERIMENTS

We were able to compare experimental growth rate data to both forms of the kinetic model. Using the color shift method [11], the TiO_2 film growth rate was measured as a function of time during the pulse, as in equation (9). The growth rate for the whole process was determined from measurement of the final film thickness and compared to equation (17). Figure 4 shows the results for both instantaneous and integrated growth rate. The fact that the growth rate data exhibit reasonably good agreement with the experimental data is taken as evidence that the assumption of a well-mixed reactor for Pulsed-MOCVD is valid.

3.1. *Growth rate during the pulse*

During some experiments with particularly rapid deposition rate, it was possible to measure the growth rate during each pulse. The most rapid growth rate was observed for high precursor concentration and moderate substrate temperature, $c_{mo} = 5.4\%$ and $T = 525°\mathrm{C}$. Figure 4(a) shows the growth rate measurements through the pulse period for this

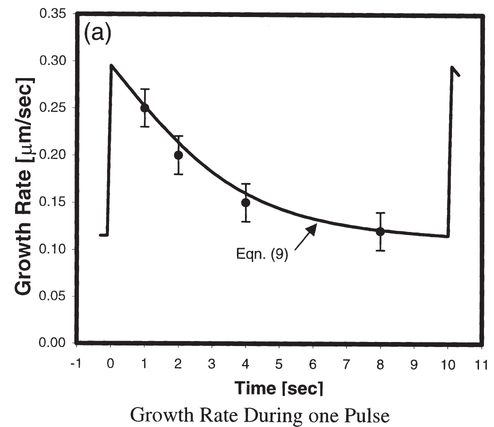

Growth Rate During one Pulse

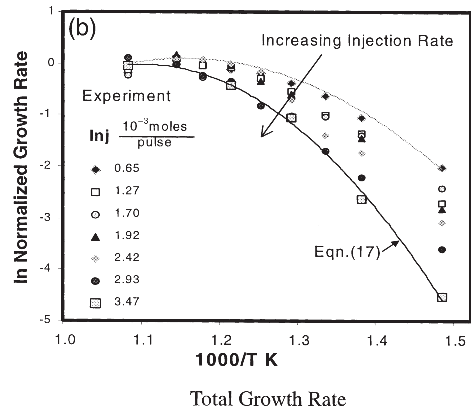

Total Growth Rate

Fig. 4. Comparison of experimental growth rate measurements to kinetic model. (a) Growth rate vs time during one pulse, equation (9), (b) Arrhenius plot of total normalized growth rate per pulse, equation (17), for all ranges of precursor injection rate.

experiment. The kinetic model for instantaneous growth rate, equation (9), was used to simulate the oxide film growth through a pulse. The model demonstrates the expected growth behavior. The following values for TiO_2 deposition from TTIP were used:

$\tau_{10} = 10^{-14}$ s	$\tau_{30} = 10^{-9}$ s
$T_v = (290 + 10t)$ K	$M = 0.2843$ kg/mole
$\sigma^{mo} = 6.25\times10^{-19}$ m^2	$\Omega_{ox} = 3.115\times10^{-29}$ m^3
$E_A = 95$ kJ/mole K	$Q = 55$ kJ/mole K
$\alpha = 0.9$	$c_{mo} = 5.4\%$ mol
$t_p = 10$ s	$\tau_p = 2.65$ s
$P_{max} = 14$ torr	$P_{min} = 3$ torr

3.2. *Process growth rate*

The film growth rate measurements for more than 60 experiments over a range of precursor injection rate were used to evaluate the integrated form of the kinetic model, equation (17). Figure 4(b) shows the normalized growth rate on an Arrhenius plot over all injection rates. The growth rate data were normalized using the maximum possible growth rate for 100% conversion efficiency [10]. The growth rate exhibits kinetic control at temperatures below 550°C. The growth rate becomes limited by the precursor supply rate in the temperature range between 550°C and 650°C, where conversion efficiency typically approaches 100%.

The normalized growth rate appears to exhibit a change in activation energy with increasing injection rate. This effect is the result of the other activated process, physical adsorption, which depends on precursor vapor partial pressure and surface temperature. Examination of the limiting cases for high and low injection rate reveals that the decreased effective activation energy for low injection rate is indeed due to the adsorption mechanism. For the limiting case of high injection rate in the kinetic range (low temperature), the normalized growth rate would be a function of the decomposition reaction rate:

$$\mathrm{NGR}(T_s) = \int_0^{t_p} \frac{\exp(-E_A/RT_s)}{c_{mo}P(t)k_2(t)}\mathrm{d}t \qquad (18)$$

$$c_{mo}P(t)k_2(t) \gg k_1, k_3$$

For the other limiting case of low temperature and low injection rate, the model predicts an effective activation energy which is equal to the reaction energy minus adsorption energy.

$$\mathrm{NGR}(T_s) = \int_0^{t_p} \frac{k_1}{k_3}\mathrm{d}t = \int_0^{t_p} \exp(-(E_A - Q)/RT_s)\mathrm{d}t$$

$$c_{mo}P(t)k_2(t) \ll k_1 < k_3 \qquad (19)$$

Following this analysis, the apparent activation energies for the highest and lowest injection rate experiments can be determined from the data in Fig. 4(b). The limiting case of high injection rate yields an activation energy of 110±10 kJ/g-mole. The apparent activation energy for the low injection rate case is found to be 60±10 kJ/g-mole. Using equation (19), the adsorption energy, Q, is found to be on the order of 50±10 kJ/g-mole, which is in the range expected for physical adsorption [11]. When these values are used in equation (17) the model gives a good approximation of the experiment as seen in Fig. 4(b).

4. CONCLUSION

The phenomenological model describing the reaction kinetics of the growing film was derived from a Langmuir model of the mass balance on the growing film surface. The growth rate was normalized by the molecular arrival rate, making the normalized growth rate model a very general result, applicable to many types of single precursor deposition systems. Both forms of the model, for growth rate at a given temperature and precursor concentration with time, and for normalized growth rate as a function of surface temperature and molar injection rate demonstrated good agreement with the experimental results. This agreement indicates the validity of the assumption that the Pulsed-MOCVD system operates as a well-mixed reactor. The mixing of the vapor in the reactor and the unsteady nature of the process result in conversion efficiencies and process control not normally encountered in conventional CVD.

In future research, the model will be used to scale up the Pulsed-MOCVD process to deposit 6–10 μm thick solid films of yttria-stabilized-zirconia (YSZ) on porous nickel oxide–YSZ samples for proof of concept research in low cost fabrication of solid oxide fuel cells (SOFCs).

Acknowledgements—This research was supported by the National Science Foundation under Grant No. DMI-9796114. Dr. Krumdieck also received support from an ARCS Foundation Scholarship and an SAE Doctoral Scholars Award. The pulsed ultrasonic nozzle method was developed in collaboration with, and with contribution from, Dr. Harvey Berger, Sono-Tek Corporation, Milton, NY [8]. The Pulsed-MOCVD kinetic deposition model was developed with a major contribution from Professor Rishi Raj, University of Colorado at Boulder.

REFERENCES

1. Jensen, K. F., in *Chemical Vapor Deposition Principles and Applications*, ed. M. L. Hitchman and K. F. Jensen. Academic Press, London, 1993.
2. Kelkar, A. S., Mahajan, R. L. and Sani, R. L., *Trans. ASME*, 1996, **118**, 814.
3. Akiyama, Y., Sato, T. and Imaishi, N., *J. Crystal Growth*, 1995, **147**, 130.
4. Siefering, K. L. and Griffin, G. L., *J. Electrochem. Soc.*, 1990, **137**(3), 1207.

5. Fictorie, C. P., Evans, J. F. and Gladfelter, W. L., *J. Vac. Sci. Technol. A*, 1994, **12**(4), 1108.
6. Masi, M., Zonca, R. and Carra, S., *J. Electrochem. Soc.*, 1999, **146**(1), 103.
7. Jones, A. C., Leedham, T. J., Wright, P. J., Crosbie, M. J., Lane, P. A., Williams, D. J., Fleeting, K. A., Otway, D. J. and O'Brien, P., *Chem. Vap. Deposition*, 1998, **4**, 46.
8. US Patent No. 5,451,260. CRF D-1394-Raj, *et al*. Sono-Tek Corp. Licensee, 1986.
9. Morosanu, C. E., *Thin Films by Chemical Vapor Deposition*. Elsevier, Amsterdam, 1990.
10. Krumdieck, S. and Raj, R., *J. Am. Ceram. Soc.*, 1999, **82**(6), 1605.
11. Krumdieck, S. P., Dissertation, University of Colorado at Boulder, 1999.
12. Adamson, A. W., *Adsorption of Gases and Vapors on Solids in Physical Chemistry of Surfaces*. Wiley, New York, 1982 (chapter XVI).